

# Mechanics of Irregular Honeycomb Structures

**Sondipon Adhikari**

Zienkiewicz Centre for Computational Engineering, College of Engineering, Swansea University, Bay  
Campus, Swansea, Wales, UK, Email: [S.Adhikari@swansea.ac.uk](mailto:S.Adhikari@swansea.ac.uk)  
Twitter: [@ProfAdhikari](https://twitter.com/ProfAdhikari), Web: <http://engweb.swan.ac.uk/~adhikaris>

Advances in AEROSPACE ENGINEERING

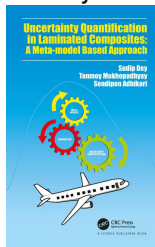
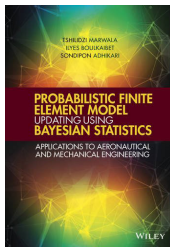
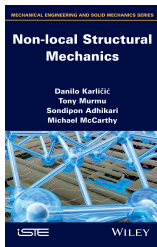
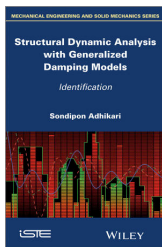
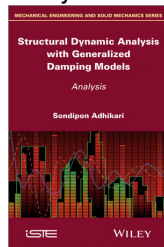
Indian Institute of Engineering Science and Technology, Shibpur, India  
19-20 March 2021







- *Development* of fundamental computational methods for structural dynamics and uncertainty quantification
  - A. Dynamics of complex systems
  - B. Inverse problems for linear and non-linear dynamics
  - C. Uncertainty quantification in computational mechanics
- *Applications* of computational mechanics to emerging multidisciplinary research areas
  - D. Vibration energy harvesting / dynamics of wind turbines
  - E. Dynamics and mechanics of metamaterials and multi-scale systems



## 1 Introduction

- A brief history of metamaterials
- Regular lattices
- Irregular lattices

## 2 Formulation for the viscoelastic analysis

## 3 Equivalent elastic properties of randomly irregular lattices

## 4 Effective properties of irregular lattices: uncorrelated uncertainty

- General results - closed-form expressions
- Special case 1: Only spatial variation of the material properties
- Special case 2: Only geometric irregularities
- Special case 3: Regular hexagonal lattices

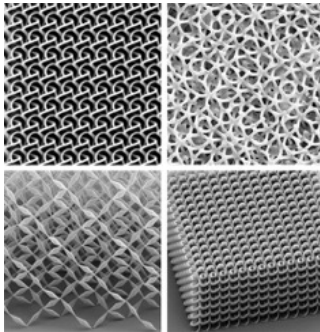
## 5 Effective properties of irregular lattices: correlated uncertainty

## 6 Results and discussions

- Spatially correlated irregular elastic lattices
- Viscoelastic properties of regular lattices
- Spatially correlated irregular viscoelastic lattices

## 7 Conclusions

- Metamaterials are **designer media** with periodic units comprised of unique tailor-made geometry and pattern aimed at accomplishing exceptional and unusual bulk properties which are unprecedented in conventional materials.
- Mechanical metamaterials achieve their **unusual effective properties** from the geometry and structure, and not from the intrinsic property of the constitutive material.
- An essential feature of metamaterials, operating in any frequency ranges or of any length-scales, is the **periodicity of a unit cell**:



- In 1898, **Jagdish Chandra Bose** conducted the **first microwave experiment on twisted structures**. These twisted structures match the geometries that are known as artificial chiral media in today's terminology. He also researched double refraction (birefringence) in crystals. Other research included polarization of electric field "waves" that crystals produce. He discovered this type of polarization in other materials including a class of dielectrics.
- The origin of modern metamaterials was in field of *electromagnetism* and ideas can be traced back to 1967 from Russia.
- However, it was the seminal papers by Smith et al. in 2000 demonstrating **negative** permeability and permittivity by a periodic array of split-ring resonators, and by Pendry (2000) demonstrating the **perfect lens** that started the current interest in metamaterials.
- Since then several concepts and devices have been conceived which **challenge conventional physical laws**, such as negative refraction, and invisibility cloaking in electromagnetism and optics.
- These **extraordinary developments** not only attracted researchers but also captured the imagination of the public and in some cases, science fiction.

- The next round of development was in *acoustic* metamaterials exploiting the idea of locally resonant behaviour.
- The consideration of sub-wavelength structures opened up immense possibilities, including *negative* effective elastic modulus, *negative* density (or mass), or both, anisotropy in the effective mass or density and *non-reciprocal* response.
- The *mechanical* metamaterials emerged following in the footsteps of electromagnetic and acoustic metamaterials, primarily within the past 10 years.
- *Intense research* in recent years shows ultralight metamaterials approaching theoretical strength limit, pentamode materials with cloaking mode, negative refraction elastic waves, elastic cloaking and hyperbolic elastic metamaterials.



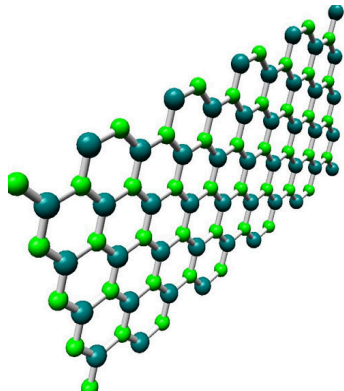
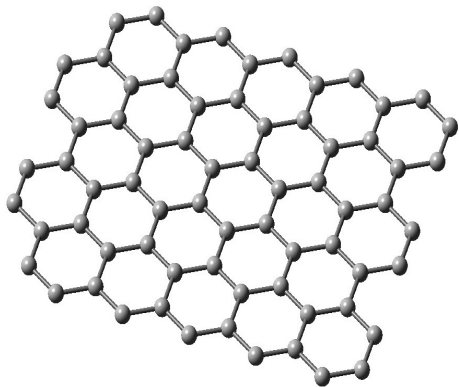
- The **rise of mechanical metamaterials** coincides with remarkable recent advances in manufacturing technology and 3D printing.
- From the point of view of analytical techniques, **two distinct type** of metamaterials are considered, namely, (1) static mechanical metamaterials and (2) dynamic mechanical metamaterials.
- The roots of static mechanical metamaterials can be traced back to late 80's with the discovery of **negative Poisson's ratio** cellular structures.
- Dynamic metamaterials differ from static metamaterials by a crucial point - it is the dynamic metamaterials which explicitly exploits sub-wavelength scale properties.
- This talk is related to **dynamic behaviour** of cellular metamaterials.
- The dynamic behaviour makes the equivalent in-plane properties **frequency dependent**.

## Hexagonal lattices in 2D

- **Lattice** based metamaterials are abundant in man-made and natural systems at various length scales.
- They are made of **periodic** identical/near-identical geometric units.
- Among various lattice geometries (triangle, square, rectangle, pentagon, hexagon), **hexagonal lattice** is most common (note that hexagon is the highest “space filling” pattern in 2D).
- This talk is about **in-plane** viscoelastic properties of 2D hexagonal lattice structures - commonly known as “honeycombs”

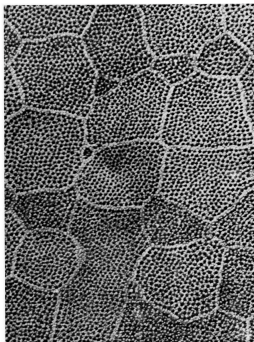
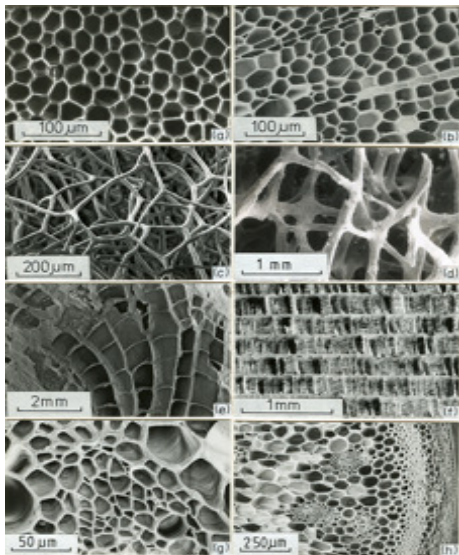


www.shutterstock.com - 113350987



Illustrations of a single layer graphene sheet and a boron nitride nano sheet

# Lattice structures - nature



Top left: cork, top right: balsa, next down left: sponge, next down right: trabecular bone, next down left: coral, next down right: cuttlefish bone, bottom left: leaf tissue, bottom right: plant stem, third column - epidermal cells (from web.mit.edu)

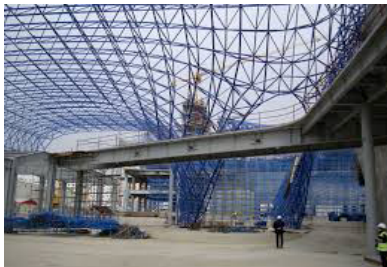
# Lattice structures - human made



(a) Automotive: BMW i3



(b) Aerospace carbon fibre



(c) Civil engineering: building frame

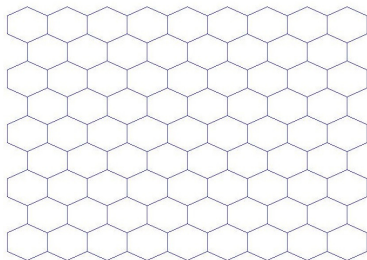


(d) Architecture

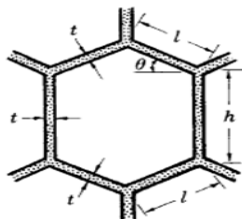
- Shall we consider lattices as “structures” or “materials” from a mechanics point of view?
- At what relative length-scale a lattice *structure* can be considered as a *material* with equivalent elastic properties?
- In what ways structural irregularities *influence* equivalent elastic / viscoelastic properties? Can we evaluate it in a quantitative as well as in a qualitative manner?
- What is the consequence of *random* structural irregularities on the homogenisation approach in general? Can we obtain statistical measures?
- How can we efficiently *compute* equivalent elastic / viscoelastic properties of random lattice structures?

- Hexagonal lattice structures have been modelled as a **continuous solid** with an equivalent elastic moduli throughout its domain.
- This approach **eliminates** the need of detail finite element modelling of lattices in complex structural systems like sandwich structures.
- Extensive amount of research has been carried out to predict the **equivalent elastic / viscoelastic properties** of regular lattices consisting of perfectly periodic hexagonal cells [39].
- Analysis of two dimensional hexagonal lattices dealing with **in-plane elastic properties** are commonly based on an unit cell approach, which is applicable only for perfectly periodic cellular structures.
- For the dynamic analysis of perfectly periodic structures, Floquet-Bloch theorem is normally employed to characterise wave propagation.

- Unit cell approach - Gibson and Ashby (1999)



(e) Regular hexagon ( $\theta = 30^\circ$ )



(f) Unit cell

- We are interested in homogenised equivalent in-plane elastic properties
- This way, we can avoid a detailed structural analysis considering all the beams and treat it as a material



## Equivalent elastic properties of regular hexagonal lattices

- The cell walls are treated as beams of thickness  $t$ , depth  $b$  and Young's modulus  $E_s$ .  $l$  and  $h$  are the lengths of inclined cell walls having inclination angle  $\theta$  and the vertical cell walls respectively.
- The equivalent elastic properties are:

$$E_1 = E_s \left(\frac{t}{l}\right)^3 \frac{\cos \theta}{\left(\frac{h}{l} + \sin \theta\right) \sin^2 \theta} \quad (1)$$

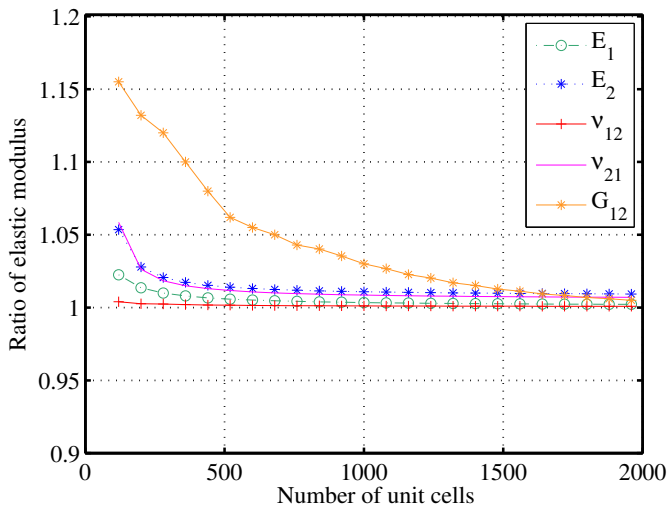
$$E_2 = E_s \left(\frac{t}{l}\right)^3 \frac{\left(\frac{h}{l} + \sin \theta\right)}{\cos^3 \theta} \quad (2)$$

$$\nu_{12} = \frac{\cos^2 \theta}{\left(\frac{h}{l} + \sin \theta\right) \sin \theta} \quad (3)$$

$$\nu_{21} = \frac{\left(\frac{h}{l} + \sin \theta\right) \sin \theta}{\cos^2 \theta} \quad (4)$$

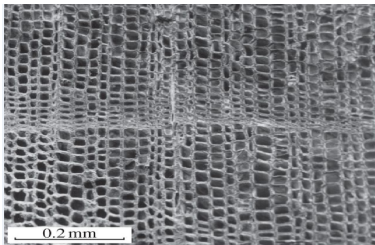
$$G_{12} = E_s \left(\frac{t}{l}\right)^3 \frac{\left(\frac{h}{l} + \sin \theta\right)}{\left(\frac{h}{l}\right)^2 \left(1 + 2\frac{h}{l}\right) \cos \theta} \quad (5)$$

- A finite element code has been developed to obtain the in-plane elastic moduli numerically for hexagonal lattices.
- Each cell wall has been modelled as an Euler-Bernoulli beam element having three degrees of freedom at each node.
- For  $E_1$  and  $\nu_{12}$ : two opposite edges parallel to direction-2 of the entire hexagonal lattice structure are considered. Along one of these two edges, uniform stress parallel to direction-1 is applied while the opposite edge is restrained against translation in direction-1. Remaining two edges (parallel to direction-1) are kept free.
- For  $E_2$  and  $\nu_{21}$ : two opposite edges parallel to direction-1 of the entire hexagonal lattice structure are considered. Along one of these two edges, uniform stress parallel to direction-2 is applied while the opposite edge is restrained against translation in direction-2. Remaining two edges (parallel to direction-2) are kept free.
- For  $G_{12}$ : uniform shear stress is applied along one edge keeping the opposite edge restrained against translation in direction-1 and 2, while the remaining two edges are kept free.



$\theta = 30^\circ$ ,  $h/l = 1.5$ . FE results converge to analytical predictions after 1681 cells.

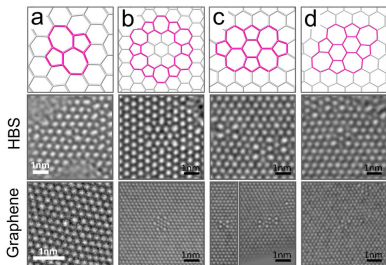
# Irregular lattice structures



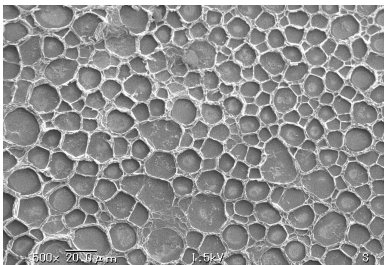
(g) Cedar wood



(h) Manufactured honeycomb core



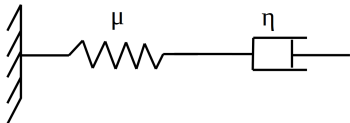
(i) Graphene image



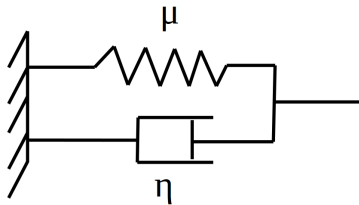
(j) Fabricated CNT surface

- A **significant limitation** of the aforementioned unit cell approach is that it cannot account for the spatial irregularity, which is practically inevitable.
- **Spatial irregularity** may occur due to manufacturing uncertainty, structural defects, variation in temperature, pre-stressing and micro-structural variabilities.
- To include the effect of irregularity, **voronoi honeycombs** have been considered in several studies.
- The effect of different forms of irregularity on elastic properties and structural responses of hexagonal lattices are generally based on **direct finite element (FE) simulation**.
- In the FE approach, a small change in geometry of a single cell may require completely new geometry and meshing of the entire structure. In general this makes the entire process **time consuming and tedious**.
- The problem becomes worse for **uncertainty quantification** of the responses, where the expensive finite element model is needed to be simulated for a large number of samples while using a Monte Carlo based approach.

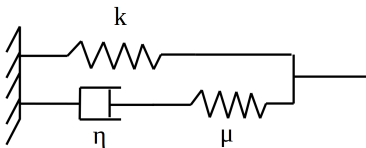
# Viscoelastic models



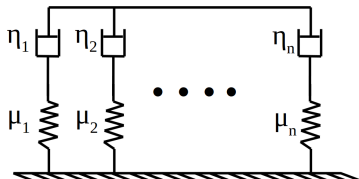
(k) Maxwell model



(l) Voigt model



(m) Standard linear model



(n) Generalised Maxwell model

**Figure:** Springs and dashpots based models viscoelastic materials.

The viscoelastic kernel function can be expressed for the four models as

■ *Maxwell model:*

$$g(t) = \mu e^{-(\mu/\eta)t} \mathcal{U}(t) \quad (6)$$

■ *Voigt model:*

$$g(t) = \eta \delta(t) + \mu \mathcal{U}(t) \quad (7)$$

■ *Standard linear model:*

$$g(t) = E_R \left[ 1 - \left( 1 - \frac{\tau_\sigma}{\tau_\epsilon} \right) e^{-t/\tau_\epsilon} \right] \mathcal{U}(t) \quad (8)$$

■ *Generalised Maxwell model:*

$$g(t) = \left[ \sum_{j=1}^n \mu_j e^{-(\mu_j/\eta_j)t} \right] \mathcal{U}(t) \quad (9)$$

Models similar to this is also known as the Pony series model.

Viscoelastic model	Complex modulus
Biot model	$G(\omega) = G_0 + \sum_{k=1}^n \frac{a_k i \omega}{i \omega + b_k}$
Fractional derivative	$G(\omega) = \frac{G_0 + G_\infty (i \omega \tau)^\beta}{1 + (i \omega \tau)^\beta}$
GHM	$G(\omega) = G_0 \left[ 1 + \sum_k \alpha_k \frac{-\omega^2 + 2i \xi_k \omega_k \omega}{-\omega^2 + 2i \xi_k \omega_k \omega + \omega_k^2} \right]$
ADF	$G(\omega) = G_0 \left[ 1 + \sum_{k=1}^n \Delta_k \frac{\omega^2 + i \omega \Omega_k}{\omega^2 + \Omega_k^2} \right]$
Step-function	$G(\omega) = G_0 \left[ 1 + \eta \frac{1 - e^{-st_0}}{st_0} \right]$
Half cosine model	$G(\omega) = G_0 \left[ 1 + \eta \frac{1 + 2(st_0/\pi)^2 - e^{-st_0}}{1 + 2(st_0/\pi)^2} \right]$
Gaussian model	$G(\omega) = G_0 \left[ 1 + \eta e^{\omega^2/4\mu} \left\{ 1 - \operatorname{erf} \left( \frac{i \omega}{2\sqrt{\mu}} \right) \right\} \right]$

Complex modulus for some viscoelastic models in the frequency domain



- We consider that each constitutive element of a hexagonal unit within the lattice structure is modelled using viscoelastic properties. For simplicity, we use Biot model with only one term. Frequency dependent complex elastic modulus for an element is expressed as

$$E(\omega) = E_S \left( 1 + \epsilon \frac{i\omega}{\mu + i\omega} \right) \quad (10)$$

where  $\mu$  and  $\epsilon$  are the relaxation parameter and a constant defining the 'strength' of viscosity, respectively.  $E_S$  is the intrinsic Young's modulus.

- The amplitude of this complex elastic modulus is given by

$$|E(\omega)| = E_S \sqrt{\frac{\mu^2 + \omega^2 (1 + \epsilon)^2}{\mu^2 + \omega^2}} \quad (11)$$

- The phase ( $\phi$ ) of this complex elastic modulus is given by

$$\phi(E(\omega)) = \tan^{-1} \left( \frac{\epsilon\mu\omega}{\mu^2 + \omega^2(1 + \epsilon)} \right) \quad (12)$$

# Mathematical idealisation of irregularity in lattice structures

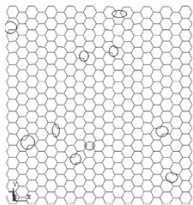


Fig. Randomly missing cell wall

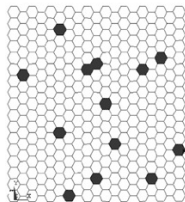


Fig. Random filled cell

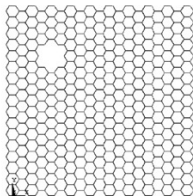
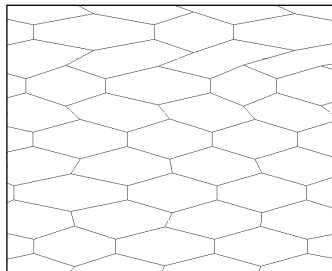
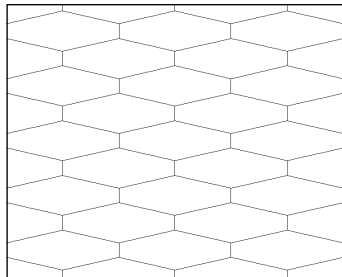


Fig. Missing cell cluster

## Irregular honeycombs



- Random spatial irregularity in cell angle is considered in this study.

- The equivalent elastic properties for a regular lattice:

$$E_1 = E_s \left( \frac{t}{l} \right)^3 \frac{\cos \theta}{\left( \frac{h}{l} + \sin \theta \right) \sin^2 \theta} \quad (13)$$

$$E_2 = E_s \left( \frac{t}{l} \right)^3 \frac{\left( \frac{h}{l} + \sin \theta \right)}{\cos^3 \theta} \quad (14)$$

$$\nu_{12} = \frac{\cos^2 \theta}{\left( \frac{h}{l} + \sin \theta \right) \sin \theta} \quad (15)$$

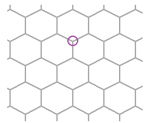
$$\nu_{21} = \frac{\left( \frac{h}{l} + \sin \theta \right) \sin \theta}{\cos^2 \theta} \quad (16)$$

$$G_{12} = E_s \left( \frac{t}{l} \right)^3 \frac{\left( \frac{h}{l} + \sin \theta \right)}{\left( \frac{h}{l} \right)^2 \left( 1 + 2 \frac{h}{l} \right) \cos \theta} \quad (17)$$

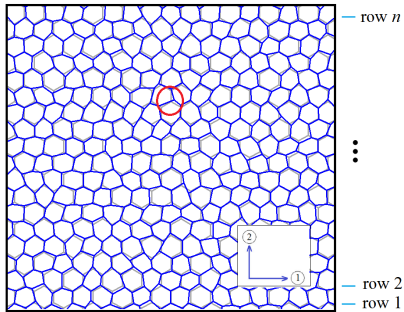
- Parameters of these expressions **CANNOT** be randomised to obtain equivalent properties for an irregular lattice.

- Direct numerical simulation to deal with irregularity in lattice structures may not necessarily provide proper understanding of the underlying physics of the system. An **analytical approach** could be a simple, insightful, yet an efficient way to obtain effective elastic properties of lattice structures.
- This work develops a structural mechanics based analytical framework for predicting equivalent in-plane elastic properties of irregular lattices having **spatially random** variations in cell angles.
- **Closed-form** analytical expressions will be derived for equivalent in-plane elastic properties.
- An approach based on the **frequency-domain** representation of the viscoelastic property of the constituent elements in the cells is used.

# The philosophy of the analytical approach for irregular lattices



(a)

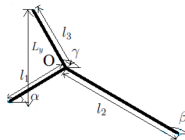
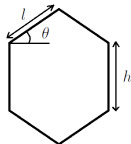


— regular honeycomb    — irregular honeycomb

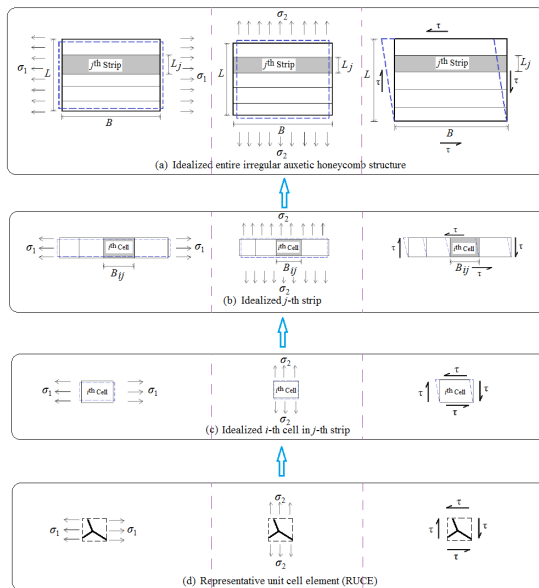
(b)

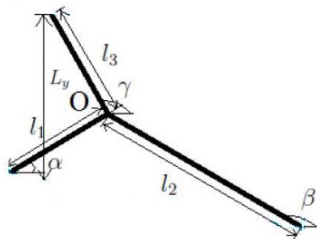
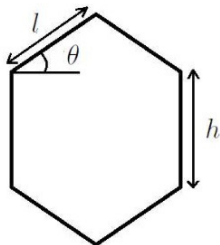


(c)



# The idealisation of RUCE and the bottom-up homogenisation approach

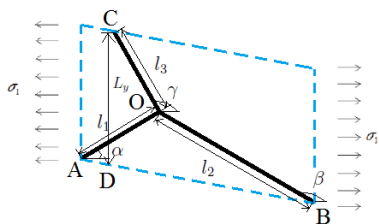




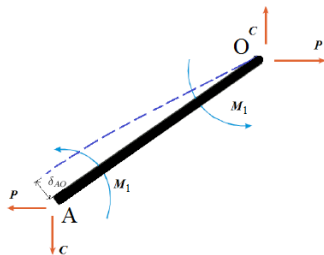
(a) Classical unit cell for regular lattices (b) Representative unit cell element (RUCE) geometry for irregular lattices



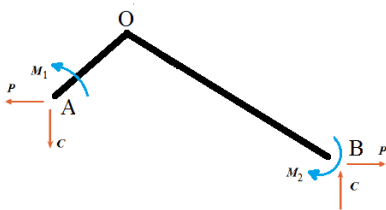
# RUCE and free-body diagram for the derivation of $E_1$



(a)



(b)



(c)

## Longitudinal Young's modulus for an idealized RUCE

- Stress  $\sigma_1$  is applied in direction-1 for deriving the expression of longitudinal Young's modulus for a single RUCE ( $E_{1U}$ ). From the condition of vertical equilibrium, it can be concluded that the vertical forces acting on points A and B should be of equal magnitude and opposite sign.
- The horizontal forces acting on points A and B can be expressed as  $P = \sigma_1 L_y b$ , where  $L_y$  represents the length CD and  $b$  is the height of honeycomb sheet (dimension perpendicular to the 1-2 plane).
- The moments  $M_1$  and  $M_2$  can be expressed as

$$M_1 = \frac{1}{2}(Pl_1 \sin \alpha - Cl_1 \cos \alpha) \quad (18)$$

$$M_2 = \frac{1}{2}(Pl_2 \sin \beta - Cl_2 \cos \beta) \quad (19)$$

- Considering the rotational equilibrium of the free-body diagram presented in, the expression for  $C$  can be obtained as

$$C = P \left( \frac{l_1 \sin \alpha - l_2 \sin \beta}{l_1 \cos \alpha - l_2 \cos \beta} \right) \quad (20)$$

- The horizontal deflection of point A with respect to point O ( $\delta_{AO}^h$ ) consists of the deflection due to force  $P$  and the force  $C$

$$\delta_{AO}^h = \left( \frac{Pl_1^3 \sin \alpha}{12E_s I} - \frac{Cl_1^3 \cos \alpha}{12E_s I} \right) \sin \alpha \quad (21)$$

where the first and second terms in the bracket represents the deflection of point A with respect to point O in the direction perpendicular to AO due to forces  $P$  and  $C$  respectively.

- The superscript  $h$  is used to represent horizontal direction of the applied stress. Here,  $E_s$  represents the intrinsic material property of the material, by which the honeycomb cell walls (/connecting members) are made of.
- The notation  $I$  represents the second moment of area of the cell walls, i.e.  $I = bt^3/12$ , where  $t$  denotes the thickness of honeycomb cell wall.

- The horizontal deflection of point B with respect to point O can be expressed as

$$\delta_{BO}^h = \left( \frac{Pl_2^3 \sin \beta}{12E_s I} - \frac{Cl_1^3 \cos \beta}{12E_s I} \right) \sin \beta \quad (22)$$

- The distance of the point vertically below joint O and on the line AB is given by

$$\delta_O = \frac{l_2 \sin \beta l_1 \cos \alpha - l_1 \sin \alpha l_2 \cos \beta}{l_1 \cos \alpha - l_2 \cos \beta} \quad (23)$$

Considering a linear strain field along the line AB, the effective horizontal deformation of the RUCE is given by

$$\begin{aligned} \delta_1^h &= \delta_{AO}^h \frac{\delta_O}{l_1 \sin \alpha} + \delta_{BO}^h \frac{\delta_O}{l_2 \sin \beta} \\ &= \frac{\sigma_1 L_y l_1^2 l_2^2 (l_1 + l_2) (\cos \alpha \sin \beta - \sin \alpha \cos \beta)^2}{E_s t^3 (l_1 \cos \alpha - l_2 \cos \beta)^2} \end{aligned} \quad (24)$$

- The strain in direction-1 can be obtained from 24 as

$$\epsilon_1^h = \frac{\sigma_1 L_y l_1^2 l_2^2 (l_1 + l_2) (\cos \alpha \sin \beta - \sin \alpha \cos \beta)^2}{E_s t^3 (l_1 \cos \alpha - l_2 \cos \beta)^3} \quad (25)$$

From 25, elastic modulus of a single RUCE in direction-1 is expressed as

$$E_{1U} = \frac{E_s t^3 (l_1 \cos \alpha - l_2 \cos \beta)^3}{L_y l_1^2 l_2^2 (l_1 + l_2) (\cos \alpha \sin \beta - \sin \alpha \cos \beta)^2} \quad (26)$$

# Longitudinal Young's modulus for a Non-idealized RUCE

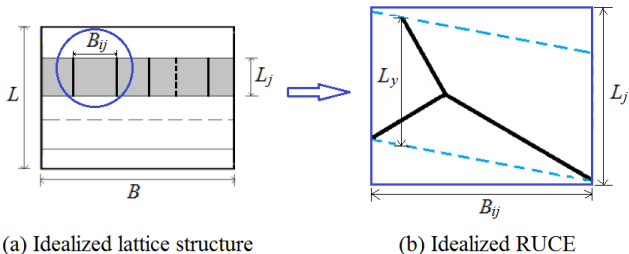


**Figure:** Idealization scheme of RUCE and the irregular lattice structure

- The expression of  $E_{1U}$  is for a non-idealized RUCE having a dimension of  $L_y$  in direction-2. However, for assembling the local properties of RUCES conveniently to the global level, it is essential to obtain the equivalent material property of an idealized RUCE ( $E'_{1U}$ ) that has a virtual dimension of  $L_j$  (dimension of the  $j^{th}$  strip in direction-2).

- Considering a linear strain field,  $E'_{1U}$  can be obtained based on the deformation compatibility condition along direction-1, i. e. the deformation of the idealized RUCE and non-idealized RUCE in direction-1 should be equal

$$\frac{PB_{ij}}{A_{NI}E'_{1U}} = \frac{PB_{ij}}{A_I E'_{1U}} \quad (27)$$

Here  $A_{NI} = L_y b$  and  $A_I = L_j b$ . The above equation can be reduced to

$$E'_{1U} = E_{1U} \frac{L_y}{L_j} \quad (28)$$

- The deformation compatibility of  $j^{\text{th}}$  strip ensures that the total deformation of the strip in direction-1 due to stress  $\sigma_1$  ( $\Delta_{1j}$ ) is the summation of individual deformations in direction-1 of each idealized RUCe ( $\Delta_{1ij}$ ), while deformation of the idealized RUCes of that strip in direction-2 are same. Thus for the  $j^{\text{th}}$  strip

$$\Delta_{1j} = \sum_{i=1}^m \Delta_{1ij} \quad (29)$$

- The 29 can be rewritten as

$$\epsilon_{1j} B_j = \sum_{i=1}^m \epsilon_{1ij} B_{ij} \quad (30)$$

where  $\epsilon_{1j}$  and  $B_j$  represent total strain and dimension in direction-1 for the  $j^{\text{th}}$  strip. Here  $B_{ij} = (l_{1ij} \cos \alpha_{ij} - l_{2ij} \cos \beta_{ij})$  and  $B_j = \sum_{i=1}^m B_{ij}$ .



- Equation (30) leads to

$$\frac{\sigma_1 B_j}{\hat{E}_{1j}} = \sum_{i=1}^m \frac{\sigma_1 B_{ij}}{E'_{1Uij}} \quad (31)$$

From 31, equivalent Young's modulus of  $j^{\text{th}}$  strip ( $\hat{E}_{1j}$ ) can be expressed as

$$\hat{E}_{1j} = \frac{B_j}{\sum_{i=1}^m \frac{B_{ij}}{E'_{1Uij}}} \quad (32)$$

where  $E'_{1Uij}$  is the equivalent longitudinal elastic modulus in direction-1 of a single idealized RUCE positioned at  $(i,j)$  that can be obtained from equation (28).

- In the next step, closed-form expression for equivalent longitudinal Young's modulus of the entire irregular lattice ( $E_{1eq}$ ) is obtained using the equivalent longitudinal Young's modulus for a single strip ( $\hat{E}_{1j}$ ).

- Employing the force equilibrium conditions and deformation compatibility condition we have

$$\sigma_1 L b = \sum_{j=1}^n \sigma_{1j} L_j b \quad (33)$$

where  $L_j$  is the dimension of  $j^{\text{th}}$  strip in direction-2 and  $L = \sum_{j=1}^n L_j$ . The notation  $b$  represents the dimension of the lattice in the perpendicular direction to 1-2 plane.

- As strains in direction-1 for each of the  $n$  strips are the same to satisfy the deformation compatibility condition, equation (33) leads to

$$E_{1eq} L = \sum_{j=1}^n \hat{E}_{1j} L_j \quad (34)$$

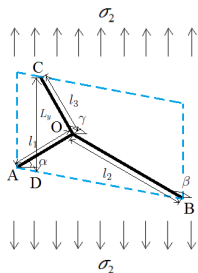
- Using 32 and 34, the equivalent Young's modulus in direction-1 of the entire irregular honeycomb structure ( $E_{1eq}$ ) can be expressed as

$$E_{1eq} = \frac{1}{L} \sum_{j=1}^n \frac{B_j L_j}{\sum_{i=1}^m \frac{B_{ij}}{E_{1Uij}}} \quad (35)$$

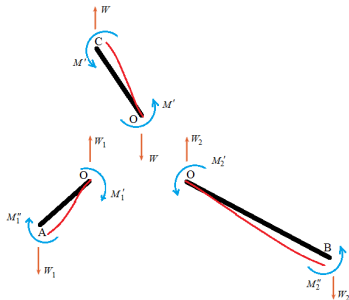
- From equations (26), (28) and (35), the expression for the longitudinal elastic modulus of the entire irregular lattice can be written as

$$E_{1eq} = \frac{E_s t^3}{L} \sum_{j=1}^n \frac{\sum_{i=1}^m (l_{1ij} \cos \alpha_{ij} - l_{2ij} \cos \beta_{ij})}{\sum_{i=1}^m \frac{l_{1ij}^2 l_{2ij}^2 (l_{1ij} + l_{2ij}) (\cos \alpha_{ij} \sin \beta_{ij} - \sin \alpha_{ij} \cos \beta_{ij})^2}{(l_{1ij} \cos \alpha_{ij} - l_{2ij} \cos \beta_{ij})^2}} \quad (36)$$

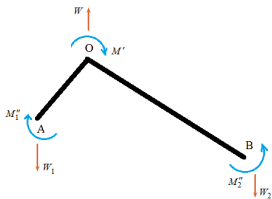
# RUCE and free-body diagram for the derivation of $E_2$



(a)

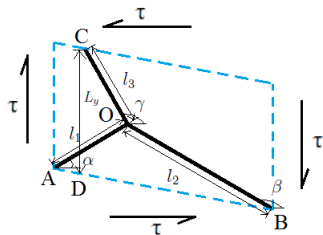


(b)

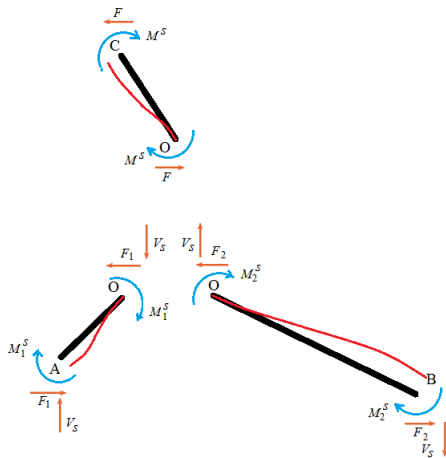


(c)

# RUCE and free-body diagram for the derivation of $G_{12}$



(a)



(b)

Equivalent  $E_1$ 

$$E_{1v}(\omega) = \frac{t^3}{L} \sum_{j=1}^n \frac{\sum_{i=1}^m (l_{1ij} \cos \alpha_{ij} - l_{2ij} \cos \beta_{ij})}{\sum_{i=1}^m \frac{l_{1ij}^2 l_{2ij}^2 (l_{1ij} + l_{2ij}) (\cos \alpha_{ij} \sin \beta_{ij} - \sin \alpha_{ij} \cos \beta_{ij})^2}{E_{sij} \left(1 + \epsilon_{ij} \frac{i\omega}{\mu_{ij} + i\omega}\right) ((l_{1ij} \cos \alpha_{ij} - l_{2ij} \cos \beta_{ij})^2)}} \quad (37)$$

 Equivalent Young's moduli  $E_2$ 

$$E_{2v}(\omega) = \frac{Lt^3}{\sum_{j=1}^n \frac{\sum_{i=1}^m (l_{1ij} \cos \alpha_{ij} - l_{2ij} \cos \beta_{ij})}{\sum_{i=1}^m E_{sij} \left(1 + \epsilon_{ij} \frac{i\omega}{\mu_{ij} + i\omega}\right) \left(l_{3ij}^2 \cos^2 \gamma_{ij} \left(l_{3ij} + \frac{l_{1ij} l_{2ij}}{l_{1ij} + l_{2ij}}\right) + \frac{l_{1ij}^2 l_{2ij}^2 (l_{1ij} + l_{2ij}) \cos^2 \alpha_{ij} \cos^2 \beta_{ij}}{(l_{1ij} \cos \alpha_{ij} - l_{2ij} \cos \beta_{ij})^2}\right)^{-1}}} \quad (38)$$

## Equivalent $G_{12}$

$$G_{12v}(\omega) = \frac{Lt^3}{\sum_{j=1}^n \frac{m}{\sum_{i=1}^m E_{sij} \left( 1 + \epsilon_{ij} \frac{i\omega}{\mu_{ij} + i\omega} \right) \left( l_{3ij}^2 \sin^2 \gamma_{ij} \left( l_{3ij} + \frac{l_{1ij}l_{2ij}}{l_{1ij}+l_{2ij}} \right) \right)^{-1}}} \quad (39)$$

### Equivalent $\nu_{12}$

$$\nu_{12eq} = -\frac{1}{L} \sum_{j=1}^n \frac{\sum_{i=1}^m (l_{ij} \cos \alpha_{ij} - l_{2ij} \cos \beta_{ij})}{\sum_{i=1}^m \frac{(\cos \alpha_{ij} \sin \beta_{ij} - \sin \alpha_{ij} \cos \beta_{ij})}{\cos \alpha_{ij} \cos \beta_{ij}}} \quad (40)$$

### Equivalent $\nu_{21}$

$$\nu_{21eq} = -\frac{L}{\sum_{j=1}^n \frac{\sum_{i=1}^m (l_{ij} \cos \alpha_{ij} - l_{2ij} \cos \beta_{ij})}{\frac{l_{1ij}^2 l_{2ij}^2 (l_{1ij} + l_{2ij}) \cos \alpha_{ij} \cos \beta_{ij} (\cos \alpha_{ij} \sin \beta_{ij} - \sin \alpha_{ij} \cos \beta_{ij})}{(l_{1ij} \cos \alpha_{ij} - l_{2ij} \cos \beta_{ij})^2 \left( l_{3ij}^2 \cos^2 \gamma_{ij} \left( l_{3ij} + \frac{l_{1ij} l_{2ij}}{l_{1ij} + l_{2ij}} \right) + \frac{l_{1ij}^2 l_{2ij}^2 (l_{1ij} + l_{2ij}) \cos^2 \alpha_{ij} \cos^2 \beta_{ij}}{(l_{1ij} \cos \alpha_{ij} - l_{2ij} \cos \beta_{ij})^2} \right)}}}} \quad (41)$$



## Only spatial variation of the material properties

- According to the notations used for a regular lattice by Gibson and Ashby (1999), the notations for lattices without any structural irregularity can be expressed as:  $L = n(h + l \sin \theta)$ ;  $l_{1ij} = l_{2ij} = l_{3ij} = l$ ;  $\alpha_{ij} = \theta$ ;  $\beta_{ij} = 180^\circ - \theta$ ;  $\gamma_{ij} = 90^\circ$ , for all  $i$  and  $j$ .
- Using these transformations in case of the spatial variation of only material properties, the closed-form formulae for compound variation of material and geometric properties (equations 37–39) can be reduced to:

$$E_{1v} = \kappa_1 \left( \frac{t}{l} \right)^3 \frac{\cos \theta}{\left( \frac{h}{l} + \sin \theta \right) \sin^2 \theta} \quad (42)$$

$$E_{2v} = \kappa_2 \left( \frac{t}{l} \right)^3 \frac{\left( \frac{h}{l} + \sin \theta \right)}{\cos^3 \theta} \quad (43)$$

$$\text{and } G_{12v} = \kappa_2 \left( \frac{t}{l} \right)^3 \frac{\left( \frac{h}{l} + \sin \theta \right)}{\left( \frac{h}{l} \right)^2 \left( 1 + 2 \frac{h}{l} \right) \cos \theta} \quad (44)$$

## Only spatial variation of the material properties

- The multiplication factors  $\kappa_1$  and  $\kappa_2$  arising due to the consideration of spatially random variation of intrinsic material properties can be expressed as

$$\kappa_1 = \frac{m}{n} \sum_{j=1}^n \frac{1}{\sum_{i=1}^m \frac{1}{E_{sij} \left( 1 + \epsilon_{ij} \frac{i\omega}{\mu_{ij} + i\omega} \right)}} \quad (45)$$

$$\text{and } \kappa_2 = \frac{n}{m} \frac{1}{\sum_{j=1}^n \frac{1}{\sum_{i=1}^m E_{sij} \left( 1 + \epsilon_{ij} \frac{i\omega}{\mu_{ij} + i\omega} \right)}} \quad (46)$$

- In the special case when  $\omega \rightarrow 0$  and there is no spatial variabilities in the material properties of the lattice, all viscoelastic material properties become identical (i.e.  $E_{sij} = E_s$ ,  $\mu_{ij} = \mu$  and  $\epsilon_{ij} = \epsilon$  for  $i = 1, 2, 3, \dots, m$  and  $j = 1, 2, 3, \dots, n$ ) and subsequently the amplitude of  $\kappa_1$  and  $\kappa_2$  becomes exactly 1. This confirms that the expressions in 45 and 46 give the necessary generalisations of the classical expressions of Gibson and Ashby (1999) through 42–44.

- In case of only spatially random variation of structural geometry but constant viscoelastic material properties (i.e.  $E_{sij} = E_S$ ,  $\mu_{ij} = \mu$  and  $\epsilon_{ij} = \epsilon$  for  $i = 1, 2, 3, \dots, m$  and  $j = 1, 2, 3, \dots, n$ ) the 37–39 lead to

$$E_{1v} = E_S \left( 1 + \epsilon \frac{i\omega}{\mu + i\omega} \right) \zeta_1 \quad (47)$$

$$E_{2v} = E_S \left( 1 + \epsilon \frac{i\omega}{\mu + i\omega} \right) \zeta_2 \quad (48)$$

$$G_{12v} = E_S \left( 1 + \epsilon \frac{i\omega}{\mu + i\omega} \right) \zeta_3 \quad (49)$$

- The random coefficients  $\zeta_i$  ( $i = 1, 2, 3$ ) are

$$\zeta_1 = \frac{t^3}{L} \sum_{j=1}^n \frac{\sum_{i=1}^m (l_{1ij} \cos \alpha_{ij} - l_{2ij} \cos \beta_{ij})}{\sum_{i=1}^m \frac{l_{1ij}^2 l_{2ij}^2 (l_{1ij} + l_{2ij}) (\cos \alpha_{ij} \sin \beta_{ij} - \sin \alpha_{ij} \cos \beta_{ij})^2}{(l_{1ij} \cos \alpha_{ij} - l_{2ij} \cos \beta_{ij})^2}} \quad (50)$$

$$\zeta_2 = \frac{Lt^3}{\sum_{j=1}^n \frac{\sum_{i=1}^m (l_{1ij} \cos \alpha_{ij} - l_{2ij} \cos \beta_{ij})}{\sum_{i=1}^m \left( l_{3ij}^2 \cos^2 \gamma_{ij} \left( l_{3ij} + \frac{l_{1ij} l_{2ij}}{l_{1ij} + l_{2ij}} \right) + \frac{l_{1ij}^2 l_{2ij}^2 (l_{1ij} + l_{2ij}) \cos^2 \alpha_{ij} \cos^2 \beta_{ij}}{(l_{1ij} \cos \alpha_{ij} - l_{2ij} \cos \beta_{ij})^2} \right)^{-1}}} \quad (51)$$

$$\zeta_3 = \frac{Lt^3}{\sum_{j=1}^n \frac{\sum_{i=1}^m (l_{1ij} \cos \alpha_{ij} - l_{2ij} \cos \beta_{ij})}{\sum_{i=1}^m \left( l_{3ij}^2 \sin^2 \gamma_{ij} \left( l_{3ij} + \frac{l_{1ij} l_{2ij}}{l_{1ij} + l_{2ij}} \right) \right)^{-1}}} \quad (52)$$

- The geometric notations for regular lattices can be expressed as:  
 $L = n(h + l \sin \theta)$ ;  $l_{1ij} = l_{2ij} = l_{3ij} = l$ ;  $\alpha_{ij} = \theta$ ;  $\beta_{ij} = 180^\circ - \theta$ ;  $\gamma_{ij} = 90^\circ$ , for all  $i$  and  $j$ . Using these transformations, the expressions of in-plane elastic moduli for regular hexagonal lattices (without the viscoelastic effect) can be obtained.
- The in-plane Young's moduli and shear modulus (viscosity dependent in-plane elastic properties) can be expressed as

$$E_{1v} = E_s \left( 1 + \epsilon \frac{i\omega}{\mu + i\omega} \right) \left( \frac{t}{l} \right)^3 \frac{\cos \theta}{\left( \frac{h}{l} + \sin \theta \right) \sin^2 \theta} \quad (53)$$

$$E_{2v} = E_s \left( 1 + \epsilon \frac{i\omega}{\mu + i\omega} \right) \left( \frac{t}{l} \right)^3 \frac{\left( \frac{h}{l} + \sin \theta \right)}{\cos^3 \theta} \quad (54)$$

$$G_{12v} = E_s \left( 1 + \epsilon \frac{i\omega}{\mu + i\omega} \right) \left( \frac{t}{l} \right)^3 \frac{\left( \frac{h}{l} + \sin \theta \right)}{\left( \frac{h}{l} \right)^2 \left( 1 + 2 \frac{h}{l} \right) \cos \theta} \quad (55)$$

- The amplitude of the elastic moduli obtained based on the above expressions converge to the closed-form equation provided by [39] in the limiting case of  $\omega \rightarrow 0$ .

- In the case of regular uniform lattices with  $\theta = 30^\circ$ , we have

$$E_{1v} = E_{2v} = 2.3E_S \left( 1 + \epsilon \frac{i\omega}{\mu + i\omega} \right) \left( \frac{t}{l} \right)^3 \quad (56)$$

- Similarly, in the case of shear modulus for regular uniform lattices ( $\theta = 30^\circ$ )

$$G_{12v} = 0.57E_S \left( 1 + \epsilon \frac{i\omega}{\mu + i\omega} \right) \left( \frac{t}{l} \right)^3 \quad (57)$$

- Regular viscoelastic lattices satisfy the reciprocal theorem

$$E_{2v}\nu_{12v} = E_{1v}\nu_{21v} = E_S \left( 1 + \epsilon \frac{i\omega}{\mu + i\omega} \right) \left( \frac{t}{l} \right)^3 \frac{1}{\sin \theta \cos \theta} \quad (58)$$

- Correlated structural and material attributes can be modelled random fields  $\mathcal{H}(\mathbf{x}, \theta)$ .
- The traditional way of dealing with random field is to discretise the random field into finite number of random variables. The available schemes for discretising random fields can be broadly divided into three groups: (1) point discretisation (e.g., midpoint method, shape function method, integration point method, optimal linear estimate method); (2) average discretisation method (e.g., spatial average, weighted integral method), and (3) series expansion method (e.g., orthogonal series expansion).
- An advantageous alternative for discretising  $\mathcal{H}(\mathbf{x}, \theta)$  is to represent it in a generalised Fourier type of series as, often termed as Karhunen-Loève (KL) expansion.

## Karhunen-Loève (KL) expansion

- Suppose,  $\mathcal{H}(\mathbf{x}, \theta)$  is a random field with covariance function  $\Gamma_{\mathcal{H}}(\mathbf{x}_1, \mathbf{x}_2)$  defined in the probability space  $(\Theta, \mathcal{F}, \mathcal{P})$ . The KL expansion for  $\mathcal{H}(\mathbf{x}, \theta)$  takes the following form

$$\mathcal{H}(\mathbf{x}, \theta) = \bar{\mathcal{H}}(\mathbf{x}) + \sum_{i=1}^{\infty} \sqrt{\lambda_i} \xi_i(\theta) \psi_i(\mathbf{x}) \quad (59)$$

where  $\{\xi_i(\theta)\}$  is a set of uncorrelated random variables.

- $\{\lambda_i\}$  and  $\{\psi_i(\mathbf{x})\}$  are the eigenvalues and eigenfunctions of the covariance kernel  $\Gamma_{\mathcal{H}}(\mathbf{x}_1, \mathbf{x}_2)$ , satisfying the integral equation

$$\int_{\mathbb{R}^N} \Gamma_{\mathcal{H}}(\mathbf{x}_1, \mathbf{x}_2) \psi_i(\mathbf{x}_1) d\mathbf{x}_1 = \lambda_i \psi_i(\mathbf{x}_2) \quad (60)$$

- In practise, the infinite series of 59 must be truncated, yielding a truncated KL approximation

$$\tilde{\mathcal{H}}(\mathbf{x}, \theta) \cong \bar{\mathcal{H}}(\mathbf{x}) + \sum_{i=1}^M \sqrt{\lambda_i} \xi_i(\theta) \psi_i(\mathbf{x}) \quad (61)$$



- Gaussian and lognormal random fields have been considered. The covariance function is represented as:

$$\Gamma_{\alpha z} = \sigma_{\alpha z}^2 e^{(-|y_1 - y_2|/b_y) + (-|z_1 - z_2|/b_z)} \quad (62)$$

where  $b_y$  and  $b_z$  are the correlation parameters at  $y$  and  $z$  directions (that corresponds to direction - 1 and direction - 2 respectively). These quantities control the rate at which the covariance decays.

- In a two dimensional physical space the eigensolutions of the covariance function are obtained by solving the integral equation analytically

$$\lambda_i \psi_i(y_2, z_2) = \int_{-a_1}^{a_1} \int_{-a_2}^{a_2} \Gamma(y_1, z_1; y_2, z_2) \psi_i(y_1, z_1) dy_1 dz_1 \quad (63)$$

where  $-a_1 \leq y \leq a_1$  and  $-a_2 \leq z \leq a_2$ .

- Assume the eigen-solutions are separable in  $y$  and  $z$  directions, i.e.

$$\psi_i(y_2, z_2) = \psi_i^{(y)}(y_2) \psi_i^{(z)}(z_2) \quad (64)$$

$$\lambda_i(y_2, z_2) = \lambda_i^{(y)}(y_2) \lambda_i^{(z)}(z_2) \quad (65)$$

## Karhunen-Loève (KL) expansion

- The solution of the integral equation reduces to the product of the solutions of two equations of the form

$$\lambda_i^{(y)} \psi_i^{(y)}(y_1) = \int_{-a_1}^{a_1} e^{(-|y_1 - y_2|/b_y)} \psi_i^{(y)}(y_2) dy_2 \quad (66)$$

- The solution of this equation, which is the eigensolution (eigenvalues and eigenfunctions) of an exponential covariance kernel for a one-dimensional random field is obtained as

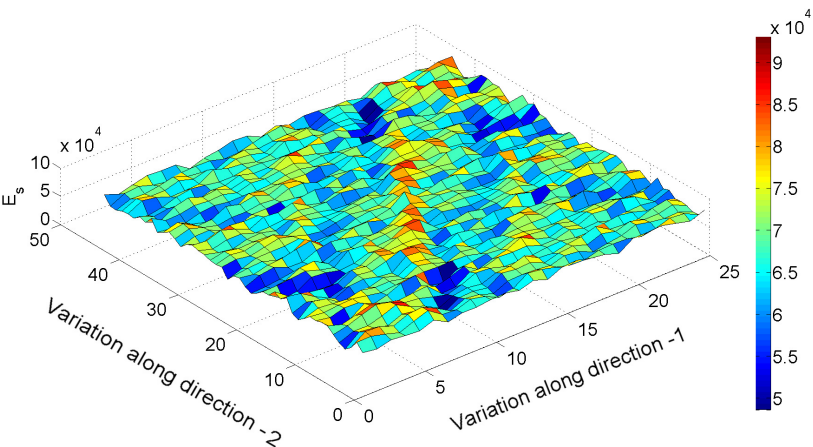
$$\begin{cases} \psi_i(\zeta) = \frac{\cos(\omega_i \zeta)}{\sqrt{a + \frac{\sin(2\omega_i a)}{2\omega_i}}} & \lambda_i = \frac{2\sigma_{\alpha_z}^2 b}{\omega_i^2 + b^2} \quad \text{for } i \text{ odd} \\ \psi_i(\zeta) = \frac{\sin(\omega_i^* \zeta)}{\sqrt{a - \frac{\sin(2\omega_i^* a)}{2\omega_i^*}}} & \lambda_i^* = \frac{2\sigma_{\alpha_z}^2 b}{\omega_i^{*2} + b^2} \quad \text{for } i \text{ even} \end{cases} \quad (67)$$

where  $b = 1/b_y$  or  $1/b_z$  and  $a = a_1$  or  $a_2$ .  $\zeta$  can be either  $y$  or  $z$  and  $\omega_i$  presents the period of the random field.

- The final eigenfunctions are given by

$$\psi_k(y, z) = \psi_i^{(y)}(y) \psi_i^{(z)}(z) \quad (68)$$

## Samples of the random fields



Spatial variability of the intrinsic elastic modulus ( $E_s$ ) with  $\Delta_m = 0.002$

## The degree of geometric irregularity

- To define the degree of irregularity, it is assumed that each connecting node of the lattice moves randomly within a certain radius ( $r_d$ ) around the respective node corresponding to the regular deterministic configuration. For physically realistic variabilities, it is considered that a given node do not cross a neighbouring node, that is

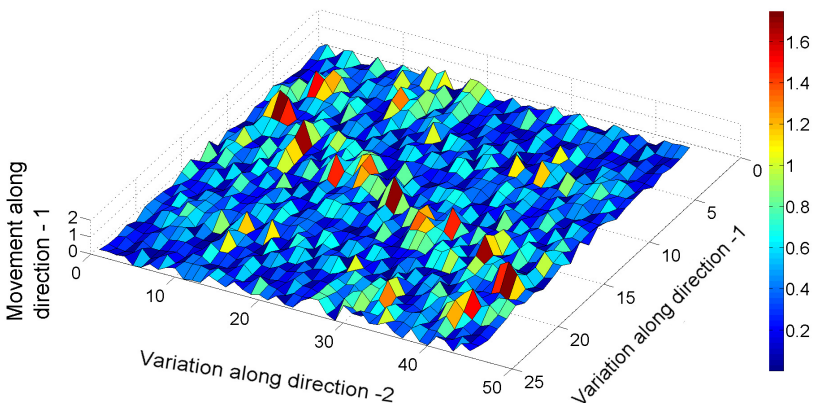
$$r_d < \min \left( \frac{h}{2}, \frac{l}{2}, l \cos \theta \right) \quad (69)$$

- In each realization of the Monte Carlo simulation, all the nodes of the lattice move simultaneously to new random locations within the specified circular bounds. Thus, the degree of irregularity ( $r$ ) is defined as a non-dimensional ratio of the area of the circle and the area of one regular hexagonal unit as

$$r = \frac{\pi r_d^2 \times 100}{2l \cos \theta (h + l \sin \theta)} \quad (70)$$

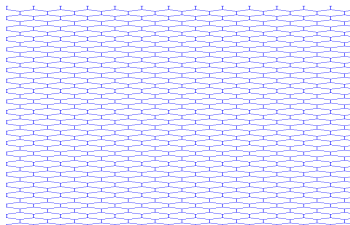
- The degree of irregularity ( $r$ ) has been expressed as percentage values for presenting the results.

## Samples of the random fields

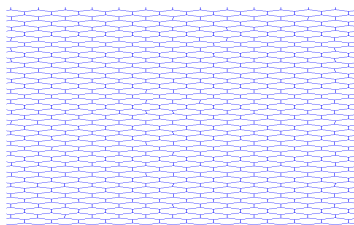


Movement of the top vertices of a tessellating hexagonal unit cell with respect to the corresponding deterministic locations ( $r = 6$ )

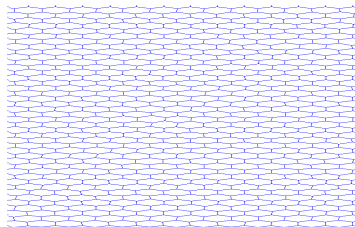
# Random geometric configurations



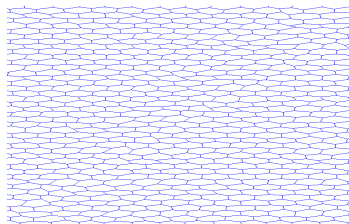
(a)




(b)



(c)



(d)

Structural configurations for a single random realisation of an irregular hexagonal lattice considering deterministic cell angle  $\theta = 30^\circ$  and  $h/l = 1$ : (a)   $r = 0$  (b)  $r = 2$  (c)  $r = 4$  (d)  $r = 6$

## Samples of random geometric configurations

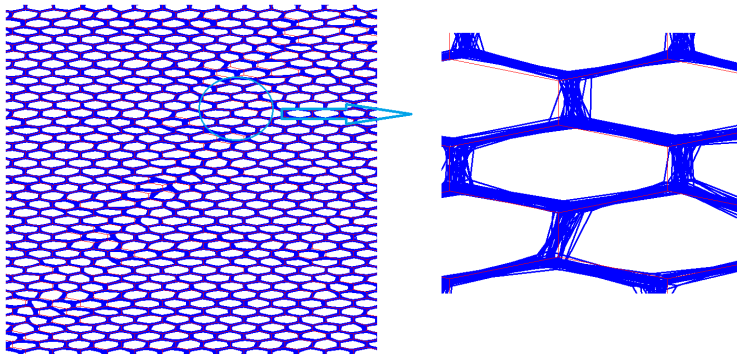


**Figure:** Simulation bound of the structural configuration of an irregular hexagonal lattice for multiple random realisations considering  $\theta = 30^\circ$ ,  $h/l = 1$  and  $r = 6$ . The regular configuration is presented using red colour.

## Samples of random geometric configurations

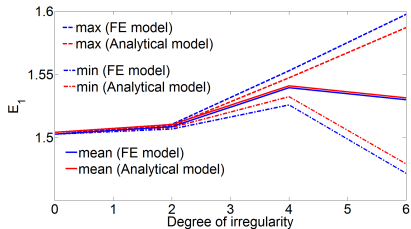
- In randomly inhomogeneous correlated system, spatial variability of the stochastic structural attributes are accounted, wherein each sample of the Monte Carlo simulation includes the spatially random distribution of structural and materials attributes with a rule of correlation.
- The spatial variability in structural and material properties ( $E_s$ ,  $\mu$  and  $\epsilon$ ) are physically attributed by **degree of structural irregularity ( $r$ )** and **degree of material property variation ( $\Delta_m$ )** respectively.
- As the two Young's moduli and shear modulus for low density lattices are proportional to  $E_s\rho^3$  [40], the **non-dimensional results** for in-plane elastic moduli  $E_1$ ,  $E_2$ , and  $G_{12}$ , unless otherwise mentioned, are presented as:

$$\bar{E}_1 = \frac{E_{1eq}}{E_s\rho^3}, \quad \bar{E}_2 = \frac{E_{2eq}}{E_s\rho^3}$$
$$\bar{G}_{12} = \frac{G_{12eq}}{E_s\rho^3}$$

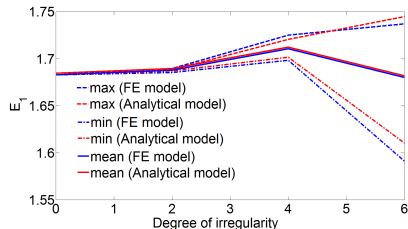
- $\rho$  is the relative density of the lattice (defined as a ratio of the planar area of solid to the total planar area of the lattice).



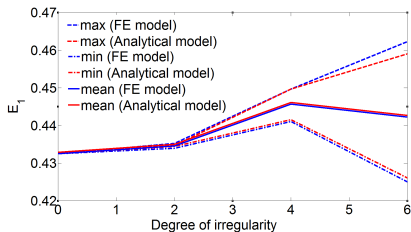
# Spatially correlated irregular elastic lattices: $E_1$



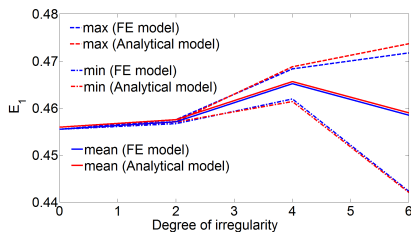
(a)  $\theta = 30^\circ$ ;  $h/l = 1$



(b)  $\theta = 30^\circ$ ;  $h/l = 1.5$



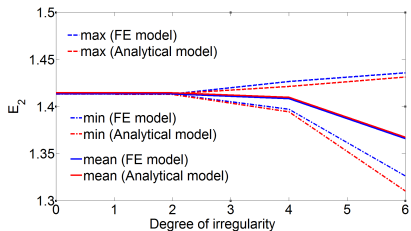
(c)  $\theta = 45^\circ$ ;  $h/l = 1$



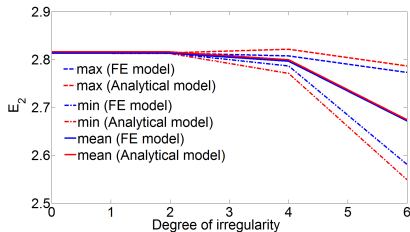
(d)  $\theta = 45^\circ$ ;  $h/l = 1.5$

**Figure:** Effective Young's modulus ( $E_1$ ) of irregular lattices

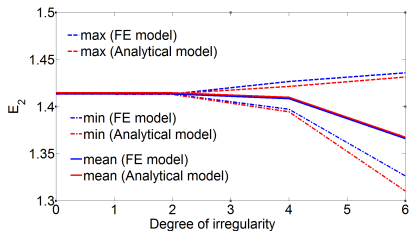
# Spatially correlated irregular elastic lattices: $E_2$



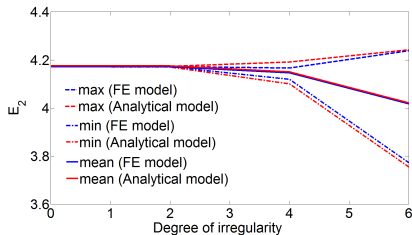
(a)  $\theta = 30^\circ$ ;  $\frac{h}{l} = 1$



(b)  $\theta = 30^\circ$ ;  $\frac{h}{l} = 1.5$



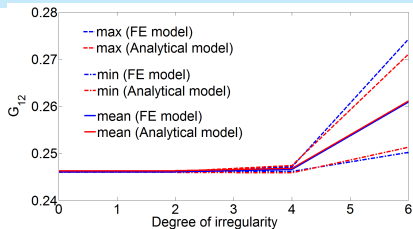
(c)  $\theta = 45^\circ$ ;  $\frac{h}{l} = 1$



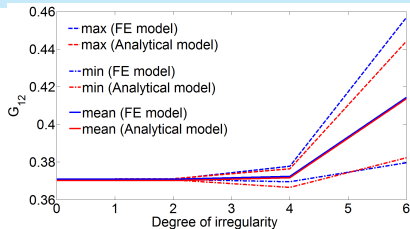
(d)  $\theta = 45^\circ$ ;  $\frac{h}{l} = 1.5$

**Figure:** Effective Young's modulus ( $E_2$ ) of irregular lattices with different structural

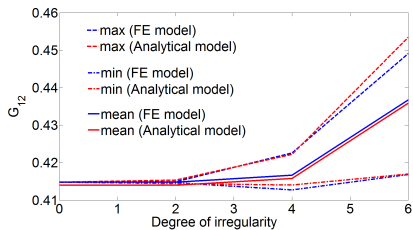
# Spatially correlated irregular elastic lattices: $G_{12}$



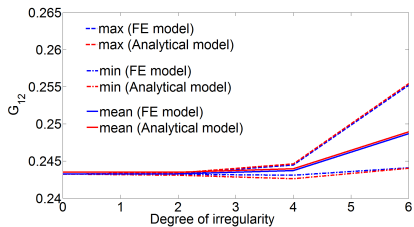
(a)  $\theta = 30^\circ$ ;  $\frac{h}{l} = 1$



(b)  $\theta = 30^\circ$ ;  $\frac{h}{l} = 1.5$



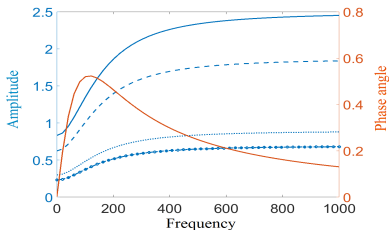
(c)  $\theta = 45^\circ$ ;  $\frac{h}{l} = 1$



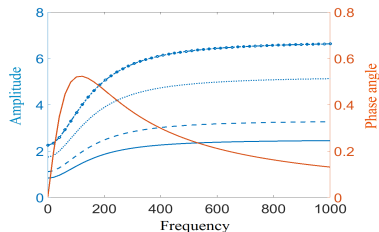
(d)  $\theta = 45^\circ$ ;  $\frac{h}{l} = 1.5$

**Figure:** Effective shear modulus ( $G_{12}$ ) of irregular lattices with different structural configurations considering correlated attributes

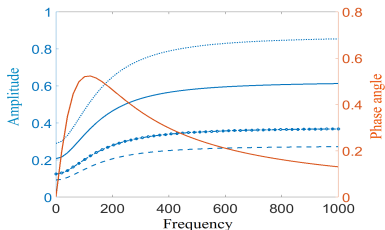
# Viscoelastic properties of regular lattices: $E_1, E_2, G_{12}$



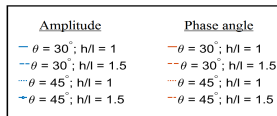
(a)



(b)

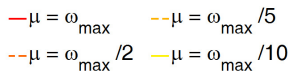
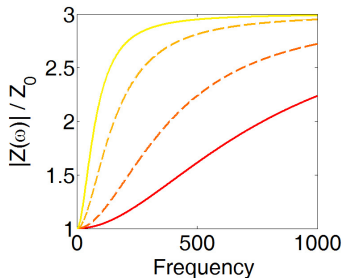


(c)

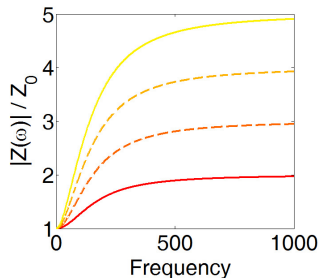


(a) Effect of viscoelasticity on the magnitude and phase angle of  $E_1$  for regular hexagonal lattices (b) Effect of viscoelasticity on the magnitude and phase angle of  $E_2$  for regular hexagonal lattices (c) Effect of viscoelasticity on the magnitude and phase angle of  $G_{12}$  for regular hexagonal lattices

# Viscoelastic properties of regular lattices



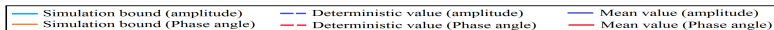
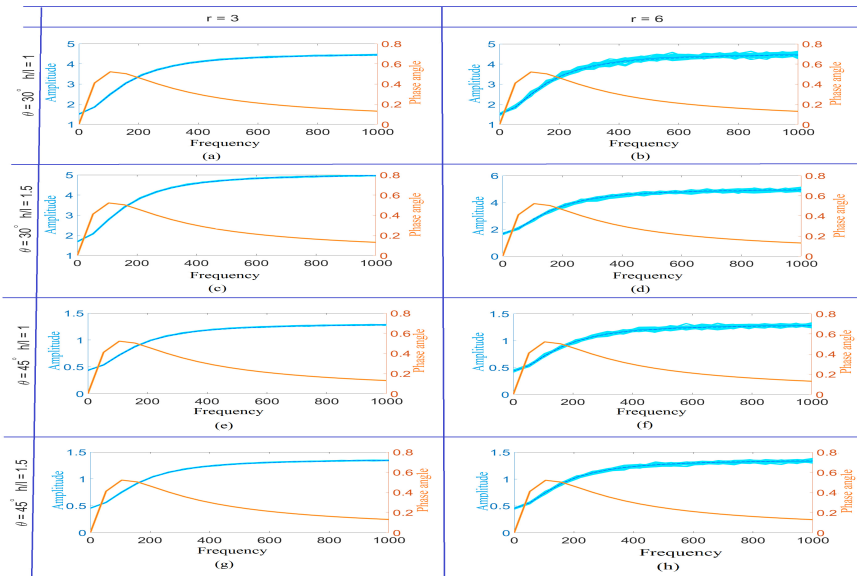
(a)



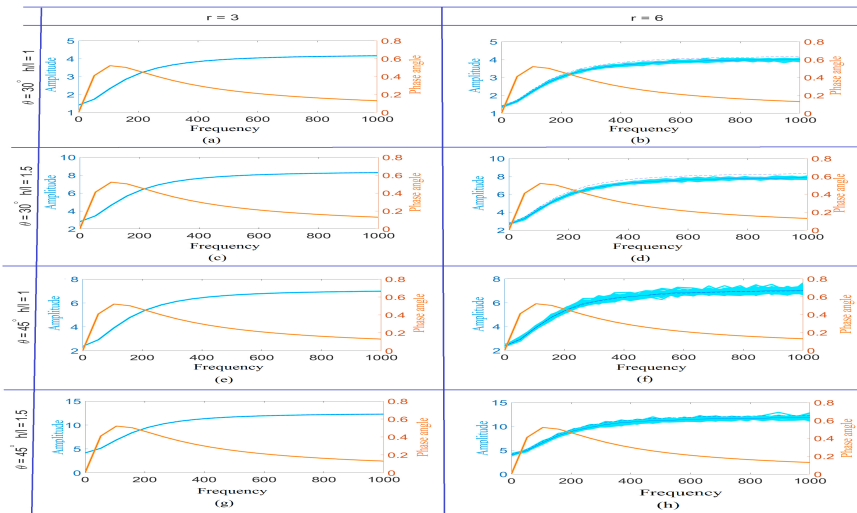
(b)

(a) Effect of variation of  $\mu$  on the viscoelastic modulus of regular hexagonal lattices (considering a constant value of  $\epsilon = 2$ ) (b) Effect of variation of  $\epsilon$  on the viscoelastic modulus of regular hexagonal lattices (considering a constant value of  $\mu = \omega_{\max} / 5$ ). Here  $Z$  represents the viscoelastic moduli (i.e.  $E_1$ ,  $E_2$  and  $G_{12}$ ) and  $Z_0$  is the corresponding elastic modulus value for  $\omega = 0$ .

# Spatially correlated irregular viscoelastic lattices: $E_1$



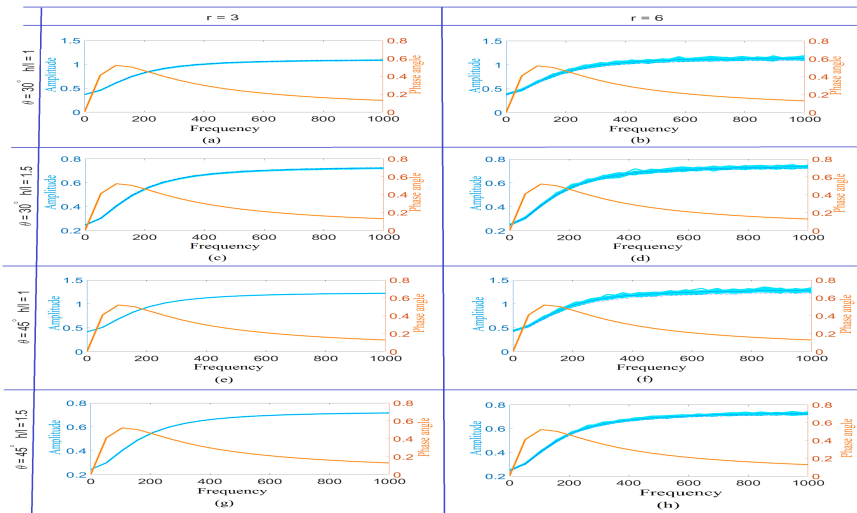
# Spatially correlated irregular viscoelastic lattices: $E_2$



— Simulation bound (amplitude)     - - - Deterministic value (amplitude)     — Mean value (amplitude)  
— Simulation bound (Phase angle)     - - - Deterministic value (Phase angle)     — Mean value (Phase angle)



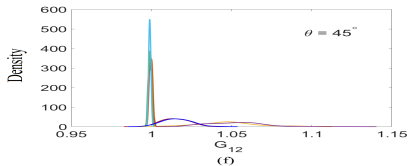
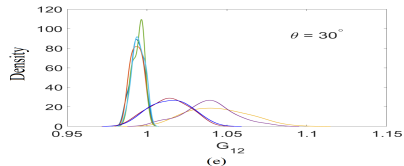
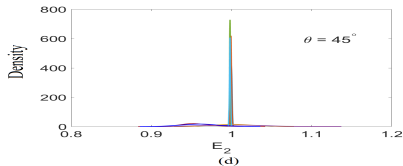
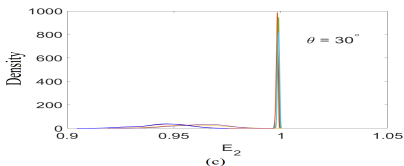
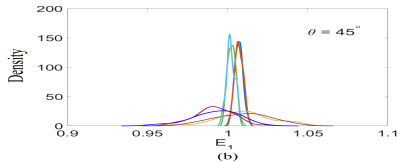
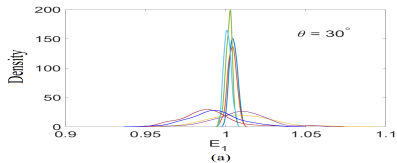
# Spatially correlated irregular elastic lattices: $G_{12}$



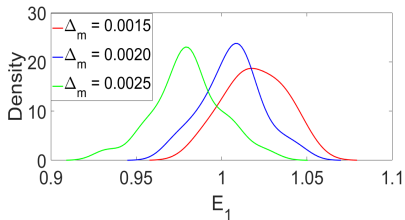
— Simulation bound (amplitude)     - - - Deterministic value (amplitude)     — Mean value (amplitude)  
— Simulation bound (Phase angle)     - - - Deterministic value (Phase angle)     — Mean value (Phase angle)



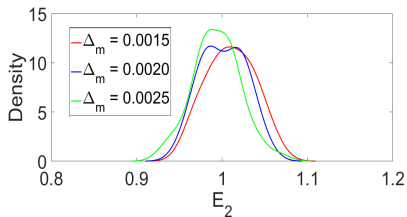
# Probability density function: random geometry



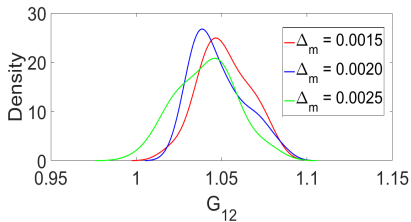
# Probability density function: random material property



(a)



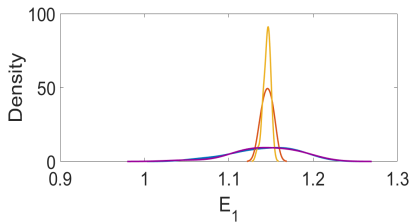
(b)



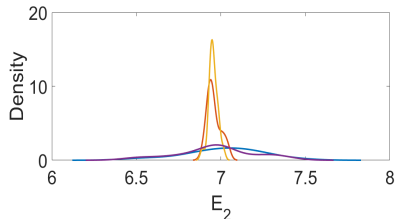
(c)

Probability density function plots for the amplitude of the elastic moduli considering randomly inhomogeneous form of stochasticity for different values of  $\Delta_m$  (i.e. coefficient of variation for spatially random correlated material properties, such as  $E_S$ ,  $\mu$  and  $\epsilon$ ). Results are presented as a ratio of the values corresponding to irregular configurations and respective deterministic values (for a frequency of 800 Hz).

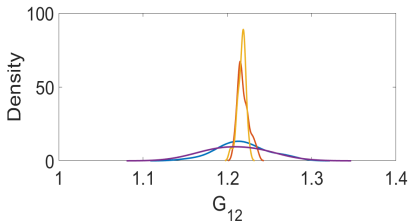
# Combined material and geometric uncertainty



(a)



(b)



(c)

- Stochasticity in structural attributes
- Stochasticity in intrinsic elastic modulus ( $E_s$ )
- Stochasticity in viscoelastic parameters ( $\mu$  and  $\epsilon$ )
- Combined stochasticity

Probabilistic descriptions for the amplitudes of three effective viscoelastic properties corresponding to a frequency of 800 Hz considering individual and compound effect of stochasticity in material and structural attributes with  $\Delta_{COV} = 0.006$



- The effect of viscoelasticity on irregular hexagonal lattices is investigated in frequency domain considering two different forms of irregularity in structural and material parameters (spatially uncorrelated and correlated).
- Spatially correlated structural and material attributes are considered to account for the effect of randomly inhomogeneous form of irregularity based on Karhunen-Loève expansion.
- The two Young's moduli and shear modulus are dependent on the viscoelastic parameters. Two in-plane Poisson's ratios depend only on structural geometry of the lattice structure.
- Using the principle of basic structural mechanics on a newly defined unit cell with a homogenisation technique, closed-form expressions have been obtained for  $E_1$ ,  $E_2$ ,  $\nu_{12}$ ,  $\nu_{21}$  and  $G_{12}$ .
- The classical closed-form expressions for equivalent in-plane elastic properties of regular hexagonal lattice structures have been generalised to consider geometric and material irregularity and viscoelastic effect.
- The new results reduce to classical formulae of Gibson and Ashby for the special case of no irregularities, no viscoelastic effect and the static limit.

# Closed-form expressions: Elastic Moduli of disordered viscoelastic lattice

$$E_{1V}(\omega) = \frac{t^3}{L} \sum_{j=1}^n \frac{\sum_{i=1}^m (l_{1ij} \cos \alpha_{ij} - l_{2ij} \cos \beta_{ij})}{\sum_{i=1}^m \frac{l_{1ij}^2 l_{2ij}^2 (l_{1ij} + l_{2ij}) (\cos \alpha_{ij} \sin \beta_{ij} - \sin \alpha_{ij} \cos \beta_{ij})^2}{E_{sij} \left(1 + \epsilon_{ij} \frac{i\omega}{\mu_{ij} + i\omega}\right) (l_{1ij} \cos \alpha_{ij} - l_{2ij} \cos \beta_{ij})^2}} \quad (71)$$

$$E_{2V}(\omega) = \frac{Lt^3}{\sum_{j=1}^n \frac{\sum_{i=1}^m (l_{1ij} \cos \alpha_{ij} - l_{2ij} \cos \beta_{ij})}{\sum_{i=1}^m E_{sij} \left(1 + \epsilon_{ij} \frac{i\omega}{\mu_{ij} + i\omega}\right) \left( l_{3ij}^2 \cos^2 \gamma_{ij} \left( l_{3ij} + \frac{l_{1ij} l_{2ij}}{l_{1ij} + l_{2ij}} \right) + \frac{l_{1ij}^2 l_{2ij}^2 (l_{1ij} + l_{2ij}) \cos^2 \alpha_{ij} \cos^2 \beta_{ij}}{(l_{1ij} \cos \alpha_{ij} - l_{2ij} \cos \beta_{ij})^2} \right)^{-1}}} \quad (72)$$

$$G_{12V}(\omega) = \frac{Lt^3}{\sum_{j=1}^n \frac{\sum_{i=1}^m (l_{1ij} \cos \alpha_{ij} - l_{2ij} \cos \beta_{ij})}{\sum_{i=1}^m E_{sij} \left(1 + \epsilon_{ij} \frac{i\omega}{\mu_{ij} + i\omega}\right) \left( l_{3ij}^2 \sin^2 \gamma_{ij} \left( l_{3ij} + \frac{l_{1ij} l_{2ij}}{l_{1ij} + l_{2ij}} \right) \right)^{-1}}} \quad (73)$$

# Closed-form expressions: Poisson's ratios of disordered viscoelastic lattice

$$\nu_{12eq} = -\frac{1}{L} \sum_{j=1}^n \frac{\sum_{i=1}^m (l_{1ij} \cos \alpha_{ij} - l_{2ij} \cos \beta_{ij})}{\sum_{i=1}^m \frac{(\cos \alpha_{ij} \sin \beta_{ij} - \sin \alpha_{ij} \cos \beta_{ij})}{\cos \alpha_{ij} \cos \beta_{ij}}} \quad (74)$$

$$\nu_{21eq} = -\frac{L}{\sum_{j=1}^n \frac{\sum_{i=1}^m (l_{1ij} \cos \alpha_{ij} - l_{2ij} \cos \beta_{ij})}{\frac{l_{1ij}^2 l_{2ij}^2 (l_{1ij} + l_{2ij}) \cos \alpha_{ij} \cos \beta_{ij} (\cos \alpha_{ij} \sin \beta_{ij} - \sin \alpha_{ij} \cos \beta_{ij})}{(l_{1ij} \cos \alpha_{ij} - l_{2ij} \cos \beta_{ij})^2 \left( l_{3ij}^2 \cos^2 \gamma_{ij} \left( l_{3ij} + \frac{l_{1ij} l_{2ij}}{l_{1ij} + l_{2ij}} \right) + \frac{l_{1ij}^2 l_{2ij}^2 (l_{1ij} + l_{2ij}) \cos^2 \alpha_{ij} \cos^2 \beta_{ij}}{(l_{1ij} \cos \alpha_{ij} - l_{2ij} \cos \beta_{ij})^2} \right)}}}} \quad (75)$$

# Some of our papers on this topic - 1

- 1 Adhikari, S., Mukhopadhyay, T., and Liu, X., "Broadband dynamic elastic moduli of honeycomb lattice materials: A generalized analytical approach", [Mechanics of Materials](#), in press.
- 2 Dwivedi, A., Banerjee, A., Adhikari, S. and Bhattacharya, B., "Optimal electromechanical bandgaps in piezo-embedded mechanical metamaterials", [International Journal of Mechanics and Materials in Design](#), in press.
- 3 Cajic, M., Karlicic, D., Paunovic, S. and Adhikari, S., "Bloch waves in parallelly connected periodic slender structures", [Mechanical Systems and Signal Processing](#), 155[6] (2021), pp. 107591.
- 4 Singh, A., Mukhopadhyay, T., Adhikari, S. and Bhattacharya, B., "Voltage-dependent modulation of elastic moduli in lattice metamaterials: Emergence of a programmable state-transition capability", [International Journal of Solids and Structures](#), 208-209[1] (2021), pp. 31-48.
- 5 Karlicic, D., Cajic, M., Chatterjee, T. and Adhikari, S., "Wave propagation in mass embedded and pre-stressed hexagonal lattices", [Composite Structures](#), 256[1] (2021), pp. 113087.
- 6 Gupta, V., Adhikari, S., Bhattacharya, B., "Exploring the dynamics of hourglass shaped lattice metastructures", [Nature Scientific Reports](#), 10[12] (2020), pp. 20943.
- 7 Mukhopadhyay, T., Naskar, S. and Adhikari, S., "Anisotropy tailoring in geometrically isotropic multi-material lattices", [Extreme Mechanics Letters](#), 40[10] (2020), pp. 100934.
- 8 Cajic, M., Karlicic, D., Paunovic, S. and Adhikari, S., "A fractional calculus approach to metadamping in phononic crystals and acoustic metamaterials", [Theoretical and Applied Mechanics](#), 47[1] (2020), pp. 81-97.
- 9 Adhikari, S., Mukhopadhyay, T., Shaw, A. and Lavery, N. P., "Apparent negative values of Young's moduli of lattice materials under dynamic conditions", [International Journal of Engineering Science](#), 150[5] (2020), pp. 103231.
- 10 Chandra, Y., Saavedra Flores, E. I. and Adhikari, S., "Buckling of 2D nano hetero structures with moire patterns", [Computational Materials Science](#), 177[5] (2020), pp. 109507.
- 11 Chandra, Y., Mukhopadhyay, T., Adhikari, S., and Figiel, L., "Size-dependent dynamic characteristics of graphene based multi-layer nano hetero-structures", [Nanotechnology](#), 31[14] (2020), pp. 145705.
- 12 Mukhopadhyay, T., Adhikari, S., and Alu, A., "Theoretical limits for negative elastic moduli in subacoustic lattice materials", [Physical Review B](#), Vol. 99, 2019, pp. 094108.
- 13 Mukhopadhyay, T., Adhikari, S., and Alu, A., "Probing the frequency-dependent elastic moduli of lattice materials", [Acta Materialia](#), Vol. 165, No. 2, 2019, pp. 654-665.

## Some of our papers on this topic - 2

- 14 Mukhopadhyay, T., Adhikari, S., and Batou, A., "Viscoelastic mechanical properties of irregular quasi-periodic lattices with spatially correlated material and structural attributes", [International Journal of Mechanical Science](#), Vol. 150, No. 1, 2019, pp. 784-806.
- 15 Mukhopadhyay, T., Mahata, T., Adhikari, S., and Zaeem, M. A., "Probing the shear modulus of two-dimensional multiplanar nanostructures and heterostructures", [Nanoscale](#), Vol. 10, No. 11, 2018, pp. 5280-5294.
- 16 Mukhopadhyay, T., Mahata, A., Adhikari, S. and Asle Zaeem, M., "Effective mechanical properties of multilayer nano-heterostructures", [Nature Scientific Reports](#), (2017), pp. 15818:1-13.
- 17 Mukhopadhyay, T. and Adhikari, S., "Effective in-plane elastic properties of quasi-random spatially irregular hexagonal lattices", [International Journal of Engineering Science](#) 119 (2017), pp. 142-179.
- 18 Mukhopadhyay, T., Mahata, A., Asle Zaeem, M. and Adhikari, S., "Effective elastic properties of two dimensional multiplanar hexagonal nano-structures", [2D Materials](#), 4[2] (2017), pp. 025006:1-15.
- 19 Mukhopadhyay, T. and Adhikari, S., "Stochastic mechanics of metamaterials", [Composite Structures](#), 162[2] (2017), pp. 85-97.
- 20 Mukhopadhyay, T. and Adhikari, S., "Free vibration of sandwich panels with randomly irregular honeycomb core", [ASCE Journal of Engineering Mechanics](#), 141[6] (2016), pp. 06016008:1-5.
- 21 Mukhopadhyay, T. and Adhikari, S., "Equivalent in-plane elastic properties of irregular honeycombs: An analytical approach", [International Journal of Solids and Structures](#), 91[8] (2016), pp. 169-184.
- 22 Mukhopadhyay, T. and Adhikari, S., "Effective in-plane elastic properties of auxetic honeycombs with spatial irregularity", [Mechanics of Materials](#), 95[2] (2016), pp. 204-222.



# Further reading

- [1] E. Shamonina, L. Solymar, *Metamaterials: How the subject started*, *Metamaterials* 1 (1) (2007) 12 – 18.  
URL <http://www.sciencedirect.com/science/article/pii/S1873198807000035>
- [2] S. A. Tretyakov, *A personal view on the origins and developments of the metamaterial concept*, *Journal of Optics* 19 (1) (2017) 013002.  
URL <http://stacks.iop.org/2040-8986/19/i=1/a=013002>
- [3] F. Monticone, A. Alù, *Metamaterial, plasmonic and nanophotonic devices*, *Reports on Progress in Physics* 80 (3) (2017) 036401.  
URL <http://stacks.iop.org/0034-4885/80/i=3/a=036401>
- [4] D. R. Smith, W. J. Padilla, D. C. Vier, S. C. Nemat-Nasser, S. Schultz, *Composite medium with simultaneously negative permeability and permittivity*, *Physical Review Letters* 84 (2000) 4184–4187. doi:10.1103/PhysRevLett.84.4184.  
URL <https://link.aps.org/doi/10.1103/PhysRevLett.84.4184>
- [5] R. A. Shelby, D. R. Smith, S. Schultz, *Experimental verification of a negative index of refraction*, *Science* 292 (5514) (2001) 77–79.  
arXiv:<http://science.sciencemag.org/content/292/5514/77.full.pdf>, doi:10.1126/science.1058847.  
URL <http://science.sciencemag.org/content/292/5514/77>
- [6] J. B. Pendry, *Negative refraction makes a perfect lens*, *Physical Review Letters* 85 (2000) 3966–3969. doi:10.1103/PhysRevLett.85.3966.  
URL <https://link.aps.org/doi/10.1103/PhysRevLett.85.3966>
- [7] J. B. Pendry, *A chiral route to negative refraction*, *Science* 306 (5700) (2004) 1353–1355.  
arXiv:<http://science.sciencemag.org/content/306/5700/1353.full.pdf>, doi:10.1126/science.1104467.  
URL <http://science.sciencemag.org/content/306/5700/1353>
- [8] H. Chen, C. T. Chan, P. Sheng, *Transformation optics and metamaterials*, *Nature Materials* 9 (5) (2010) 387–396.
- [9] Y. Liu, X. Zhang, *Metamaterials: a new frontier of science and technology*, *Chem. Soc. Rev.* 40 (2011) 2494–2507.
- [10] D. Schurig, J. J. Mock, B. J. Justice, S. A. Cummer, J. B. Pendry, A. F. Starr, D. R. Smith, *Metamaterial electromagnetic cloak at microwave frequencies*, *Science* 314 (5801) (2006) 977–980. doi:10.1126/science.1133628.
- [11] S. A. Cummer, J. Christensen, A. Alù, *Controlling sound with acoustic metamaterials*, *Nature Reviews Materials* 1 (2016) 16001 EP.
- [12] P. A. Deymier, *Acoustic Metamaterials and Phononic Crystals*, *Springer Series in Solid-State Sciences*, Vol. 173, Springer, New York, USA, 2013.
- [13] Z. Liu, X. Zhang, Y. Mao, Y. Y. Zhu, Z. Yang, C. T. Chan, P. Sheng, *Locally resonant sonic materials*, *Science* 289 (5485) (2000) 1734–1736.  
arXiv:<http://science.sciencemag.org/content/289/5485/1734.full.pdf>, doi:10.1126/science.289.5485.1734.  
URL <http://science.sciencemag.org/content/289/5485/1734>
- [14] R. Halir, P. J. Bock, P. Cheben, A. Ortega-Monux, C. Alonso-Ramos, J. H. Schmid, J. Lapointe, D.-X. Xu, J. G. Wanguemert-Perez, I. Molina-Fernandez, S. Janz, *Waveguide sub-wavelength structures: a review of principles and applications*, *Laser & Photonics Reviews* 9 (1) (2015) 25–49. doi:10.1002/lpor.201400083.  
URL <http://dx.doi.org/10.1002/lpor.201400083>
- [15] N. Fang, D. Xi, J. Xu, M. Ambati, W. Srituravanich, C. Sun, X. Zhang, *Ultrasonic metamaterials with negative modulus*, *Nature Materials* 5 (6) (2006) 452–456.
- [16] Z. Yang, J. Mei, M. Yang, N. H. Chan, P. Sheng, *Membrane-type acoustic metamaterial with negative dynamic mass*, *Physical Review Letters* 101 (2008) 204301. doi:10.1103/PhysRevLett.101.204301.  
URL <https://link.aps.org/doi/10.1103/PhysRevLett.101.204301>
- [17] Y. Ding, Z. Liu, C. Qiu, J. Shi, *Metamaterial with simultaneously negative bulk modulus and mass density*, *Physical Review Letters* 99 (2007) 093904.  
doi:10.1103/PhysRevLett.99.093904.  
URL <https://link.aps.org/doi/10.1103/PhysRevLett.99.093904>
- [18] D. Torrent, J. Sanchez-Dehesa, *Anisotropic mass density by two-dimensional acoustic metamaterials*, *New Journal of Physics* 10 (2) (2008) 023004.
- [19] H. Huang, C. Sun, *Locally resonant acoustic metamaterials with 2D anisotropic effective mass density*, *Philosophical Magazine* 91 (6) (2011) 981–996.



- [20] R. Fleury, D. L. Sounas, C. F. Sieck, M. R. Haberman, A. Alù, Sound isolation and giant linear nonreciprocity in a compact acoustic circulator, *Science* 343 (6170) (2014) 516–519. doi:10.1126/science.1246957.
- [21] M.-A. Miri, E. Verhagen, A. Alù, Optomechanically induced spontaneous symmetry breaking, *Physical Review A* 95 (2017) 053822.
- [22] J. B. Pendry, D. Schurig, D. R. Smith, Controlling electromagnetic fields, *Science* 312 (5781) (2006) 1780–1782. doi:10.1126/science.1125907.
- [23] G. Ma, P. Sheng, Acoustic metamaterials: From local resonances to broad horizons, *Science Advances* 2 (2). doi:10.1126/sciadv.1501595.
- [24] A. Alù, Metamaterials: Prime time, *Nature Materials* 15 (2016) 1229–1231. doi:10.1038/nmat4814.
- [25] M. Kadic, T. Buckmann, R. Schittny, M. Wegener, Metamaterials beyond electromagnetism, *Reports on Progress in Physics* 76 (12) (2013) 126501. URL <http://stacks.iop.org/0034-4885/76/i=12/a=126501>
- [26] J. Christensen, M. Kadic, O. Kraft, M. Wegener, Vibrant times for mechanical metamaterials, *MRS Communications* 5 (3) (2015) 453–462. doi:10.1557/mrc.2015.51.
- [27] X. Li, H. Gao, Mechanical metamaterials: Smaller and stronger, *Nature Materials* 15 (4) (2016) 373–374.
- [28] A. A. Zadpoor, Mechanical meta-materials, *Mater. Horiz.* 3 (2016) 371–381. doi:10.1039/C6MH00065G. URL <http://dx.doi.org/10.1039/C6MH00065G>
- [29] X. Zheng, H. Lee, T. H. Weisgraber, M. Shusteff, J. DeOtte, E. B. Duoss, J. D. Kuntz, M. M. Biener, Q. Ge, J. A. Jackson, S. O. Kucheyev, N. X. Fang, C. M. Spadaccini, Ultralight, ultrastiff mechanical metamaterials, *Science* 344 (6190) (2014) 1373–1377.
- [30] J. B. Berger, H. N. G. Wadley, R. M. McMeeking, Mechanical metamaterials at the theoretical limit of isotropic elastic stiffness, *Nature* 543 (7646) (2017) 533–537.
- [31] M. Kadic, T. Buckmann, N. Stenger, M. Thiel, M. Wegener, On the practicability of pentamode mechanical metamaterials, *Applied Physics Letters* 100 (19) (2012) 191901.
- [32] T. Buckmann, M. Thiel, M. Kadic, R. Schittny, M. Wegener, An elasto-mechanical unfeelability cloak made of pentamode metamaterials, *Nature Communications* 5 (2014) 4130 EP –.
- [33] R. Zhu, X. N. Liu, G. K. Hu, C. T. Sun, G. L. Huang, Negative refraction of elastic waves at the deep-subwavelength scale in a single-phase metamaterial, *Nature Communications* 5 (2014) 5510 EP –.
- [34] G. W. Milton, M. Briane, J. R. Willis, On cloaking for elasticity and physical equations with a transformation invariant form, *New Journal of Physics* 8 (10) (2006) 248.
- [35] N. Stenger, M. Wilhelm, M. Wegener, Experiments on elastic cloaking in thin plates, *Physical Review Letters* 108 (2012) 014301.
- [36] V. M. Garcia-Chocano, J. Christensen, J. Sánchez-Dehesa, Negative refraction and energy funneling by hyperbolic materials: an experimental demonstration in acoustics, *Physical Review Letters* 112 (2014) 144301.
- [37] S. M. Ahmadi, S. A. Yavari, R. Wauthle, B. Pouran, J. Schrooten, H. Weinans, A. A. Zadpoor, Additively manufactured open-cell porous biomaterials made from six different space-filling unit cells: the mechanical and morphological properties, *Materials* 8 (4) (2015) 1871–1896. URL <http://www.mdpi.com/1996-1944/8/4/1871>
- [38] R. Lakes, Foam structures with a negative poisson's ratio, *Science* 235 (4792) (1987) 1038–1040.
- [39] L. Gibson, M. F. Ashby, *Cellular Solids Structure and Properties*, Cambridge University Press, Cambridge, UK, 1999.
- [40] H. X. Zhu, J. R. Hobbell, W. Miller, A. H. Windle, Effects of cell irregularity on the elastic properties of 2d voronoi honeycombs, *Journal of the Mechanics and Physics of Solids* 49 (4) (2001) 857–870.